Article:

Qiu, S. orcid.org/0000-0003-2235-1162, Zhao, S., Xu, X. et al. (8 more authors) (2025) Aggregate turnover in a dryland red soil after long-term application of chemical fertilizers or manure. Soil Use and Management, 41 (1). e70017. ISSN 0266-0032

https://doi.org/10.1111/sum.70017

Type of contribution: Original research article

Aggregate turnover in a dryland red soil after long-term application of chemical fertilizers or manure

Shaojun Qiu [1], Shicheng Zhao [1], Xinpeng Xu [1], Xiubin Wang[1], Ping He [1], Xichu Yu [2], Kailou Liu [2], Manoj Menon[3], Huiyi Yang [4], Peter Christie[1], Wei Zhou [1]

[1.] State Key Laboratory of Efficient Utilization of Arable Land in China; Key Laboratory of Plant Nutrition and Fertilizer, Ministry of Agriculture and Rural Affairs; Institute of Agricultural Resources and Regional Planning, Chinese Academy of Agricultural Sciences, Beijing 100081, China

[2.] Jiangxi Red Soil Institute, Nanchang 331717, China

[3.] Department of Geography, University of Sheffield, Sheffield, S10 2TN, United Kingdom

[4.] Natural Resources Institute, University of Greenwich, Central Avenue Chatham Maritime, Kent ME4 4TB, UK

[*] Corresponding author: S. Qiu, E-mail: qiushaojun@caas.cn; P. He, E-mail: heping02@caas.cn; Tel: +86-10-82105638; Fax: +86-10-82106206.

Abstract

Physical protection of carbon (C) in soil aggregates is an important mechanism affecting soil organic carbon (SOC) stocks but there is little information on the turnover dynamics of aggregates in dryland red soils after different long-term fertilization practices. Different aggregate size classes in zero fertilizer (CK), chemical fertilizer (CF), and chemical fertilizer combined with manure (MCF) treatments were examined. The Roth C model was used to simulate C inputs based on SOC dynamics, the carbon, aggregation, and structure turnover (CAST) model was used to evaluate soil structure and C sequestration at different aggregate size classes with time. MCF treatment significantly ($P < 0.05$) increased total macroaggregate C, and fractions of macroaggregate C compared with the other two treatments because C inputs and C sequestration rate increased significantly ($P < 0.05$) according to Roth C model simulation. The CAST model performed well in simulating the changes in soil structure and organic C stocks in different aggregate size classes with time. The simulation results indicate that particulate organic matter (POM) is the primary source of aggregate turnover, that free silt-clay particles have a more rapid turnover than the silt-clay particles in other (larger) aggregates, and that the disruption criterion for aggregate distribution in CAST model parameters followed the sequence MCF > CF > CK in the low pH and low SOC red soil. Overall, the CAST model is a good tool for simulation of aggregate dynamics in red soil under different fertilization treatments.

Keywords: soil aggregates; carbon stocks; fertilizer practices; model simulation; red soil

Introduction

Climate warming induced by increasing atmospheric carbon dioxide concentrations is widely accepted to be occurring and is an issue of increasing concern (Huesh et al., 2017; Zhou et al., 2018; Jia et al., 2020). As a consequence, C storage and sequestration potential in soils have attracted considerable interest (Carvalhais et al., 2014; Xiao et al., 2020) because the amount of C stored in soils is about twice that stored in the atmosphere (Lal, 2004). The protection of aggregate C by soil organic matter (SOM) is an important mechanism affecting SOC stock (Six and Paustian, 2014; Garland et al., 2023). Moreover, soil aggregate structure in agricultural land can be influenced by management practices such as tillage and application of chemical fertilizers or exogenous C (Zhou et al., 2022; Liu et al., 2023; Dorji et al., 2020). Understanding the mechanisms by which protected C pools respond to different fertilization practices is crucial for maximizing SOC stocks.

Different fertilization practices can affect soil aggregate quantity and quality as well as SOC and aggregate C concentrations (Lichter et al., 2008; Ramteke et al., 2024). Intensive cropping systems with high C inputs from aboveground to belowground or exogenous C application result in aggregate formation. Carbon accumulation in soils to which chemical fertilizers are applied occurs mainly in free silt and clay particles. Further manure application can increase the physically protected C and promote SOC accumulation (Glude et al., 2008; Yu et al., 2012; Wen et al., 2021). Neff et al. (2002) report that nitrogen inputs promote the decomposition of light fraction C (labile pools) and increase the stability of heavy faction C (stable pools). Besides, in agricultural systems frequent removal of aboveground production and regular tillage may lead to complex changes in SOC induced by fertilization practices in the short term, while the field located experiment with long-term fertilization practices can effectively avoid the effect of tillage and other agronomic practices, and clearly demonstrate the dynamics of SOC changes induced due to fertilization practices (Qiu et al., 2016; Schmidt et al., 2011), therefore, the effects of fertilization practices on SOC and aggregates are well illustrated by long-term fertilization experiment.

Aggregates are the structural units in soils that control SOC dynamics. The complex structure of SOM is often arbitrarily divided into labile and stable pools (Brown et al., 2014; Gulde et al., 2008). Labile SOM has a more rapid turnover than stable SOM. Particulate organic matter (POM) is usually an important labile fraction that plays an important role in short-term C cycling (Gulde et al., 2008), while stable SOC pools mainly determine the magnitude of long-term C stocks (Zhou et al., 2017). In different soil aggregates the increase in SOC is partly determined by the link between macroaggregate turnover, microaggregate formation, and C stabilization within microaggregates (Six et al, 2000). It is therefore necessary to explore the amount and the duration of C stocks in different aggregate size classes in order to clarify the effects of different aggregate size classes on SOC stocks.

Mathematical models can effectively evaluate and predicate SOC dynamics (Coleman and Jenkinson, 1999; Keating et al., 2003; Malamoud et al., 2009; Wang et al., 2013). Stamati et al. (2013) recently developed a model of coupled C, aggregation, and structural turnover (CAST) which integrates the advantages of the Struc-C model (Malamoud et al., 2009) and the RothC model (Coleman and Jenkinson, 1999). The CAST model fully considers each aggregate type as a single C pool and the input of exogenous organic materials and POM derived from the decomposition of exogenous organic materials (Li et al., 2017; Stamati et al. 2013), and the parameters and C pools in RothC model are introduced into different size aggregates in the CAST model. The CAST model also simulates the turnover rate of each aggregate size and its feedbacks on SOC dynamics. Thus, the CAST model can better explore the relationships among different aggregates in soils and the response of aggregate C dynamics to management practices and other factors.

Red soils account for 22% of the total land area in China and are characterized by low soil organic matter and available nutrient contents, poor soil structure, and high acidity and aluminum toxicity. Currently, drylands with red soils are increasingly being cultivated to meet the demand for forage maize or other high-income crops. In order to explore changes in aggregate C in dryland red soils, a soil from a dryland maize cropping system under different long-term fertilizer practices was selected to (1) explore changes in soil aggregate C under long-term applications of chemical fertilizer and a combination of chemical fertilizer and manure and (2) elucidate the turnover rate in different aggregate size classes under different long-term fertilization practices using CAST model simulations.

Materials and methods

Site description

The long-term double maize cropping system began at the site (28°15’N, 116°20’E) in the spring of 1986, and spring soybean or peanut was planted before 1986. The experimental site is located at the Red Soil Research Institute in Jiangxi province, south China. This region has a typical subtropical humid monsoon climate with an annual average temperature and precipitation of 18.1 °C and 1620 mm, respectively, from 1986 to 2014. Red soils (Ferralic Cambisols according to the FAO soil classification system) are the typical soil type. Local climatic information during the experimental period is shown in Fig. 1 and has been obtained from the meteorological station at our experimental sites in the China Meteorological Data Sharing Service System (http:// http://www.cma.gov.cn). Basic information of surface soil properties (0-20 cm depth) at the initial of the located experiment was shown in Table 1.

Table 1, Fig.1

Experimental design

The field experiment comprised three treatments in triplicate with plots 22.2 m^2 in area in a randomized complete block design. The treatments were one fertilizer treatment (CF), one treatment combining manure and fertilizer (MCF) and unamended plots as a control (CK). The fertilizer rate and cropping system are shown in Table 2. The chemical fertilizers applied were urea, triple superphosphate or calcium superphosphate, and potassium chloride and the manure used was pig manure. During the crop growth period the nitrogen (N) fertilizer application was split twice as basal fertilizer and topdressing fertilizer and the phosphorus (P), potassium (K), and manure were applied as basal fertilizers. Spring maize was sown at the beginning of April and harvested in the middle of July and then summer maize was planted and harvested at the beginning of November. The soil was ploughed after summer maize harvested.

After the crop harvest in 2014, soil samples were collected from three points in each plot, and then the fresh soil samples were immediately passed through a 5-mm sieve and air-dried. The air-dried soil samples in 2014 and 1986 were isolated with wet sieving method to analyze soil aggregates. In each treatment at the start (1986) and end (2014) of the experiment, the determined data of mass and C stock in different size class aggregates and SOC concentration with a total 24 data were input CAST model to simulate the dynamic of soil aggregates. In order to simultaneously capture the regular curves of the dynamics of the mass and C concentration in different size class aggregates, the CAST model simulation originally ran with the mean monthly historical data from 1986 to 2014 for a period of 40 years.

Table 2

Water-stable aggregate fractionation

Soil aggregate separation was conducted with size density fractionation using wet sieving according to Elliott (1986), and particulate organic matter was separated from the mixture of

POM and sand using heavy liquid according to Brown et al. (2014) and Gulde et al. (2008). As described by Elliott (1986), water stable aggregates (WSA) were separated into three size classes comprising macroaggregates (AC3) (>250 µm), free microaggregates (AC2) (250 – 53 µm), and free silt-clays (AC1) (< 53 µm) using a wet sieving method. Briefly, 80.0 g air dried soil on the top of a 250 µm sieve was submerged in deionized water for 5 min at room temperature and separated with 50 vertical movements of > 2 min. Floating material was removed with a net during submergence. The efficiency of recovery during wet sieving averaged 98.7% (range 98.2-100.7%).

The microaggregates within macroaggregates (AC2,3) (250 – 53 µm) were further isolated based on the method of Six et al. (2000). Briefly, ≤ 15.0 g of oven-dried macroaggregate subsample (AC3) was slaked for 15 min and transferred onto a 250-µm mesh screen with a transparent plastic wall and the screen was shaken in running water with 50 glass beads (4 mm in diameter) until the water became clear. The <250 µm soil slurry continued to pass through a 53-µm mesh screen by wet sieving by water stable aggregate fractionation. The remaining materials with size ranges >250 µm, 250 - 53 µm and < 53 µm were coarse particulate organic matter plus sand (cPOM + sand), AC2,3, and silt-clays within AC3 (AC1,3). The recovery efficiency was 99.4% (range 98.3-100.8%).

The AC2,3 particles comprised two parts, namely fine particulate organic matter (fPOM) and silt-clays in AC2,3 (AC1,2,3). Firstly, the oven-dried AC2,3 was shaken for 12 h with 0.5% sodium hexametaphosphate at a ratio of 1:3 (soil:liquid, w/v). The dispersed slurry was passed through a 53-µm sieve, and the > 53 µm and < 53 µm particles were fPOM + sand in AC2,3 and AC1,2,3 particles.

Finally, soil cPOM + sand and fPOM + sand in AC2,3 particles were isolated to remove the sand with sodium polytungstate at a density of 2.3 g cm^{-3} at a ratio of 1:3 (soil:liquid, w/v). Soil particles fractionated with sodium polytungstate were washed 7 -10 times with deionized water on a 20-μm mesh using a vacuum filtration device. The washed particles in this step comprised cPOM and fPOM in AC2,3 (fPOM_inAC3).

At each of the fractionation steps above the separated soil particles were oven-dried at 60 °C and then weighed on a balance with 0.01 or 0.0001 g precision. After the oven-dried soil samples were passed through a 0.15-mm sieve the C concentrations in the soil particles were determined with a CN analyzer (Macrocube, Elementar, Hanau, Germany).

In addition, the quantity and type of soil clay minerals were determined with an x-ray diffractometer (Rigaku D/MAX 2500, Tokyo, Japan). Soil texture was determined with the classical sedimentation-based pipette method. The methods for the determination of other commonly analyzed soil properties were those used by Qiu et al. (2016).

Model description

The CAST model divides soil aggregates into macroaggregates, microaggregates, and silt-clays. Macroaggregates are formed by POM which is derived from the plant litter fragment and then decomposed by microorganisms. The decomposed POM associated with silt-clay sized aggregates and polymers of microbial origin which are responsible for "gluing" the structural components of aggregates subsequently form the microaggregates within macroaggregates. Microbial activity decreases gradually with POM biodegradation and the macroaggregates become unstable because of the lack of microbially-derived polymers. New macroaggregates form and the cycle of aggregation and disaggregation continues when fresh plant residues enter the soil.

The C pools in the RothC model are adopted at each aggregate size class in the CAST model. In RothC model, the C pools are decomposable plant material (DPM), resistant plant material (RPM), microbial biomass (BIO), humified organic matter (HUM), and inert organic matter (IOM). The turnover rate of IOM is from centuries to millennia (Powlson et al., 2011) and IOM therefore acts as a resistor to decomposition in both the Roth C model and CAST models. In the CAST model, fresh plant litter is split into DPM and RPM and these fractions are fragmented to form the coarse fractions of DPM (DPMc) and RPM (RPMc) which further decompose to form the fine fractions of DPM (DPMf) and RPM (RPMf). The macroaggregates contain DPMc, RPMc, DPMf, RPMf, BIO, HUM, and IOM, the microaggregates contain DPMf, RPMf, BIO, HUM, and IOM, and the silt and clay pools are composed of HUM and IOM.

During the running of the CAST model, climatic conditions, basic soil properties, WSA distribution and organic C distribution at each aggregate size, and C inputs were input as initial parameters. The main climatic conditions, e.g. mean monthly temperature, total monthly precipitation, and total monthly evaporation were used to drive the model. The basic soil properties were silt and clay content, bulk density, soil depth and sand mass in AC3 and AC2 fractions. The WSA distributions and their C contents at the beginning of the experiment are required as the initial conditions of the aggregates and then the turnover rate is tuned to make the measured and simulated data coincidence. In the CAST model each C pool of aggregate types decomposes by a first-order process with a specific rate constant and the decomposition rate of each C pool is determined by three climatic factors (e.g. temperature, precipitation, and evaporation) through their effects on microbial activity as described by the Roth C model. With respect to the input parameters in each size aggregates at the initial condition, half of the C content in POM (POM-C) is partitioned into decomposable and resistant plant material, respectively; 5 % of the silt–clay fraction C is partitioned into BIO and the remaining silt–clay fraction C is partitioned into HUM (Stamati et al. 2013).

We simulated the crop C input data using the RothC model (version 2.1 for Windows) with changing SOC content during the experimental period. The simulated plant C input is uniformly distributed each month during crop growth. The C inputs in the CAST model were 0.370, 0.480, and 0.375 t C ha^{-1} $month^{-1}$ in the control, CF and MCF treatments from April to October during crop growth, and a manure C input of 1602 kg C ha^{-1} per season crop in the MCF treatment was added in April and July as shown in Table 1. Further details of the CAST model can be found in Li et al. (2017), Panakoulia et al. (2017), Stamati et al. (2013), and the RothC model user guide (Coleman and Jenkinson, 1999).

CAST model adjustment

In the CAST model the calibrated parameters comprise those that control 1) the turnover rates of the full cycle of C processing from plant material fragmentation to POM decomposition in aggregate fractions, 2) the relative contribution of silt-clay units and POM in the aggregate size fractions, and 3) the criteria including disruption or tilling effects on aggregate distribution, and the correction factor for silt-clay mass flow which describes silt-clay unit distribution in different aggregates.

The disruption and tilling criteria for aggregate distribution determine the starting point of different aggregate size classes by CAST model simulation. The calibrated decomposition rates of different aggregate size classes and fragmented plant materials capture the change in soil structure and organic C stocks in different aggregate size classes in a chronosequence. A correction factor is used to adjust silt-clay mass flow in each aggregate type (Stamati et al., 2013). The reciprocal value of these calibrated rate constants for aggregate formation and disaggregation are reported as turnover time (y) as shown in Table 5.

The disruption and tilling criteria for aggregate distribution were first calibrated to account for the correct timing of change in the particle distribution between the measurement and simulation time series. Secondly, the parameters for turnover rates and the proportional contribution of the components in aggregation were calibrated for year 2014 data. The calibrated parameters (turnover times) (Table 5) were the POM fractions in most cases. Finally, the correction factor values were calibrated to fine tune the mass of water-stable aggregates. The rate constants for formation of each aggregate size class from the constituent particle fractions, disaggregation of each size class of aggregate, decomposition for each pool of SOC and the values for tillage and silt-clay mass flow criteria were calibrated using a step-wise process. The calibration steps proceeded from initial values taken from the RothC handbook and literature values from published observations or model results, which were individually varied around the initial values to test sensitivity before systematically varying the value to minimize RMSE, and then testing sensitivity of RMSE to the individual calibrated values once the calibrated parameter set was complete.

Root mean square error (RMSE) and normalized RMSE (nRMSE) were employed to evaluate the performance of the CAST model using simulated values and measured values which were the values of different aggregate size classes in 2007. Agreement is considered to be good when nRMSE ≤ 20%. The equations are as follows:

$$\text{RMSE} = \sqrt{\frac{\sum_{i=1}^{n}(Si-Mi)^2}{n}}$$

$$\text{nRMSE} = \frac{\text{RMSE}}{\bar{M}} \times 100$$

Where Si is the simulated value, Mi is the measured value, n is the number of measured values, and $\bar{M}$ is the average of the measured values.

According to Jamieson et al. (1991) reported, the model shows an “excellent” performance if the nRMSE⩽10%, “good” performance if 10% < nRMSE ⩽ 20 %, “fair” performance if 20% < nRMSE ⩽ 30%, and “poor” performance if the nRMSE >30%.

Statistical analysis

Statistical analysis was performed using the SPSS 16.0 for Windows software package.

Mean values of the variables in different aggregate size classes and SOC among the three treatments were compared using least significant difference at the 5% level.

Results

Measured SOC contents in 2014, RothC simulated SOC contents in 2014, and SOC sequestration rate were significantly different ($P < 0.05$) among the three treatments (Table 3). C inputs and CO_2-C emissions in the MCF treatment significantly greater ($P < 0.05$) than in the control or the chemical fertilizer treatment.

Table 3

Compared to the control in 2014 (Table 4), AC2 and AC1 masses significantly ($P < 0.05$) decreased by 20.2 and 13.4% in MCF as well as 31.7 and 25.0% in CF treatments, AC3 and AC1,3 masses significantly ($P < 0.05$) increased by 15.0 and 40.2% in MCF as well as 9.9 and 20.6% in CF treatments. Moreover, MCF treatment significantly ($P < 0.05$) increased AC1,3, cPOM and fPOM_inAC3 masses by 16.3, 68.0 and 155.6% compared to the CF treatment.

The C concentrations in different aggregate size classes are also shown in Table 4. Compared to the control, the C concentration in AC3, AC2,3, AC1,3, AC1,2,3, and fPOM_inAC3 particles significantly ($P < 0.05$) increased by 287.9, 80.9, 87.4, 48.5 and 191.3% in MCF as well as 23.5, 30.1, 37.8, 40.9 and 17.4% in CF treatments, respectively. The MCF treatment had significantly ($P < 0.05$) higher C concentrations in SOC, AC3, AC2,3, AC1,3, AC1,2,3, cPOM_inAC3, and fPOM_inAC3 particles than the control or CF.

Table 4

The CAST model (Fig. 2) well simulated the data acquired on aggregate mass distribution and carbon stocks in different aggregate size classes in the control, CF, and MCF plots over the 29 years from the start of the field experiment in 1986 to 2014. According to the SOC stock distribution among the three treatments (Fig. 2d-f), SOC stocks increased in tandem with increases in AC3 mass and organic C in AC3 particles in the first three years and then SOC stocks increased in tandem with increasing AC2 mass and organic C in AC2 particles, as shown in the MCF treatment (Fig. 2 f). Conversely, the decrease in SOC stocks in the first few years was mainly due to the disruption of AC3 in our low C content soil (Fig. 2d, e; Table 1). In the MCF treatment (Fig. 2 i) all of the OC stocks in AC3 fractions increased and the changes in AC1,2,3 and AC1,3 were higher than those in cPOM and fPOM_inAC3.

Fig. 2

Aggregate C turnover (Table 5) occurred in most cases in the fragmentation, macroaggregates, microaggregates, plant litter pools, RPMc, RPMf, DPMc, and DPMf in AC3 aggregates, and AC1 aggregates. In the decomposition of different aggregate size classes the turnover time of RPMc and RPMf in AC3 aggregate type followed the sequence CK < CF < MCF and that of $HUM_{inAC2,3}$ and HUM_{inAC2} was CK< CF < MCF, while the turnover time of HUM_{inAC1} was CK > CF > MCF.

The correction factor (Table 5) for slit-clay mass flow was related to C content and aggregate mass flow in different aggregates. The range was 0.6 to 1.3 in all parameters in the three treatments. The correction factor for AC1 was lower than AC1,3. The order of the disruption criterion for aggregate distribution changes was MCF > CF > CK.

Table 5

The evaluation of RMSE and nRMSE between measured and simulated values was better when their values decreased (Table 6). The nRMSE value was < 20% and the RMSE value was < 1.6. The CAST model therefore well predicted the soil organic C stock distribution in different aggregates. On the whole, the evaluation of nRMSE for SOC, AC3, and AC2 between measured and simulated values was slight better than for AC1 in the three treatments.

Table 6

Discussion

1. Impact of fertilization practices on soil aggregates

The differences in SOC among the three treatments were closely related to C inputs (Table 3) as shown by the simulated C inputs using the RothC model (Table 3), sufficient C input may increase SOC stocks and C sequestration (Gattinger et al., 2012; Zhang et al., 2015). In our study the order of significance ($P < 0.05$) of SOC concentration in 2014 was MCF > CF > CK and the SOC sequestration rates in the CK and CF treatments showed C losses (negative) while that in the MCF treatment showed C accumulation (positive) (Table 3). The C loss in CF treatment was attributable that the C input from maize didn't reach the C output because of N input limitation, the optimal N input didn't generally exceed 210 kg N/ha (Qiu et al., 2015); the second reason was possible that soil acidification because of long term chemical fertilizer application suppressed maize growth in the acidic soil (Guo et al., 2010). The study soil has a low pH in the CF treatment, while the combination of manure and chemical fertilizers can restrain soil acidification and increase soil pH, resulting in pH values of 4.66, 4.42, and 5.68 in the CK, CF, and MCF treatments in 2014.

Carbon inputs from aboveground or from manure application can enhance or impede SOC stability in aggregates, further affecting aggregate formation and altering soil structure (Li et al., 2017), as shown the significantly ($P < 0.05$) increase of the mass and C concentration in AC3 in MCF treatment than the control (Table 4). The POM in AC3 is mainly derived from decomposed plant residues and responds sensitively to soil management practices (Gulde et al., 2008) and therefore sufficient manure application (Table 2) can increase POM. For instance, the study site had significantly higher cPOM and fPOM_inAC3 in the MCF treatment than in the control or CF treatment. A greater turnover rate of POM (Gulde et al., 2008) results in a lower POM pool capacity compared to the other aggregate size classes (Table 4). The mass and amount of C in microaggregates (AC2 and AC2,3) can be affected by crop residues, rhizosphere deposited C and exogenous C, and furthermore, microaggregates are regarded as an indicator of C sequestration, especially AC2,3 (Gulde et al., 2008; Six et al, 2000), as shown the mass and C concentration in AC1,2,3 and AC2,3 in the present study (Table 4). Organic substrates can contribute to the C in < 53 μm soil particles. For example, there were significant ($P < 0.05$) differences in masses and C concentrations in AC1,3 and the C concentration in AC1,2,3 among the three treatments due to the fact that < 53 μm soil particles bound into macroaggregate after exogenous C input and because of the different physical protection of AC1,2,3 and AC1,3 in macroaggregates (Gulde et al., 2008; Six et al, 2000). In addition, the significantly ($P < 0.05$) lower masses and non-significant C concentrations in AC1 in the fertilization treatments than in the control also indicate an increase in C concentration in AC1 after the application of fertilizers and/or manures (Table 4).

2. Adjustment of aggregate turnover and parameters

The simulated data in different aggregates size class in CAST model well fitted the measured data on the whole in our study soil as shown the nRMSE values in Table 6 (Jamieson et al.,1991). Water-stable aggregate mass and C stocks in different aggregates gradually approached steady state from the start of the experiment to the sampling date (Fig. 2, Table 6). POM turnover plays an important role in aggregate C turnover because the adjusted parameters mainly occurred in POM fractions (Table 5). Zeller and Danbine (2011) reported that POM was the primary N source for plants in a natural system. In plant litter pool decomposition in the CAST model parameters (Table 5), the control treatment had an obviously low turnover time of DPM and the MCF treatment had a little higher turnover time of DPM, while the opposite phenomenon can be found in the turnover time of RPM, this was because that (1) POM and N decomposition is the only N source in the control treatment, (2) manure per se has plenty of liable and resistant decomposed organic materials, which is an important source of POM in the MCF treatment, (3) plenty of chemical fertilizer N in the CF and MCF treatments can promote POM decomposition (Neff et al., 2002). In contrast, the turnover time of AC1 type decomposition is shorter than AC2 and the particles of AC2,3, because AC1 has free status in soils with a higher surface area than the other size aggregates. The large surface area readily retains applied fertilizer N (Yan et al., 2012) and the associated N further released to meet crop demand by microbial metabolism or the exchange of C and N in the rhizosphere. Therefore, the AC1 aggregates was a more important source of C and N than the other silt-clay particles in macroaggregates. In macroaggregates among the three treatments the turnover time of each fraction showed an increasing trend with C input rate, especially for HUM in macroaggregates and this is consistent with the increase in C concentration in the different macroaggregate fractions. Neff et al. (2002) reported that application of N fertilizers increased the stability of < 53 μm soil particles. Abiotic factors also play an important role in regulating soil aggregate turnover (Conant et al., 2011). For example, the disruption criterion for aggregate distribution was different in the three treatments and this may be related to soil properties and fertilization practices.

Regarding the differences in correction factors (cf) in each treatment, Stamati et al. (2013) reported that a value close to 1 denoted a linear relationship between silt-clay mass flow and OC flow, a value < 1 indicates high OC concentration hotspots induced by microaggregates, and a value > 1 indicates that substantial parts of mineral surfaces are not covered with organic matter. For example, the lower cf value in AC1 than AC1,3 in the three treatments indicates that mineral surfaces in AC1 more readily associated with organic matter than AC1,3. The increase in cf value in AC1,3 from 0.8 in the control to 1.2 in the fertilization treatments (Table 5) indicates that C inputs in the fertilization treatments promote the association between organic matter and mineral surfaces, and this improves aggregate structure and increases aggregations C content, resulting in an increase in cf value in AC1,3 in the fertilization treatments.

In addition, the chemical or physical forces between cations (e.g. Fe^{3+}, Al^{3+}, Ca^{2+}) and organic compounds or between clays and SOM particles result in changes in the different size aggregate C contents and aggregate mass (Bronick and Lal, 2005). The dominant cations in our soil were Fe^{3+} and Al^{3+}, and application of manures with high ion concentrations can alter soil properties and further affect the soil aggregates. Tillage can disrupt soil aggregate (Bronick and Lal, 2005), however, the same parameters for tillage effect on POM in CAST model (Table 5) indicated that tillage didn't affect the change of soil aggregate under different fertilization management practices in our studied soil. In the initial phase of simulation, the sharp changes in different size aggregate may be related to the C input rate (Fig. 2), for example, the low C input rate in the CK and CF treatments decreased SOC concentration from the initial to the sampling date (Table 1, 3), furthermore, the lack of C resulted in the fragmentation of macroaggregate and the formation of < 250 μm aggregates, subsequently the dynamic of the mass and C concentration in aggregates gradually stabilized because of the long-term unchanged C input rate in each fertilization practice (Fig. 2).

Conclusions

Differences in nutrient applications can result in differences in C inputs to soils and sufficient C inputs contributes significantly ($P < 0.05$) to SOC stocks, as shown by the MCF treatment which had significantly greater SOC content and SOC sequestration rate than the control or the fertilizer treatment. The combination of different fertilization practices and modeling tools well simulated soil organic carbon, aggregates, and structural turnover as time proceeded. The simulation results indicate the effects of POM on soil aggregate turnover and the response of different size aggregate classes to fertilization practices. Overall, the CAST model is a good tool for simulating the response of aggregate dynamics to different fertilization treatments in this dryland red soil.

Abbreviations

SOC: soil organic carbon, **CK:** control (no fertilizer or manure), **CF:** chemical fertilizers, **MCF:** combination of manure and chemical fertilizers, **CAST:** Carbon, Aggregation, and Structure Turnover, **WSA**: water stable aggregates, **AC3**: macroaggregates (>250 μm), **AC2**: free microaggregates (250 – 53 μm), **AC1**: free silt and clays (< 53 μm), **AC2,3**: microaggregates within macroaggregates (AC2 within AC3), **AC1,3**: AC1 in AC3, **AC1,2,3**: AC1 in AC2 within AC3, **POM**: particulate organic matter, **cPOM**: coarse POM, **fPOM**: fine POM, **DPM**: decomposable plant material, **RPM**: resistant plant material, **cDPM**: coarse DPM**, cRPM:** coarse RPM, **fDPM**: fine DPM**, fRPM:** fine RPM, **BIO**: microbial biomass, **HUM**: humified organic matter, **IOM**: inert organic matter

Acknowledgements

This research was supported by National Natural Science Foundation of China (42477383), Innovation Program of Chinese Academy of Agricultural Sciences (CAAS-CSAL-202302), the National Key Research and Development Plan (2023YFD2300400). Great thanks to Professor Dr. Steven A. Banwart from University of

Leeds for his valuable suggestions on modelling analysis.

References

Bronick, C. J., & Lal, R. (2005). Soil structure and management: A review. Geoderma, 124, 3-22.

Brown, K. H., Bach, E. M., Drijber, R. A., Hofmockel, K. S., Jeske, E. S., Sawyer, J. E., & Castellano, M. J. (2014). A long-term nitrogen fertilizer gradient has little effect on soil organic matter in a high-intensity maize production system. Global Change Biology, 20, 1339-1350.

Carvalhais, N., Forkel, M., Khomik, M., Bellarby, J., Jung, M., Migliavacca, M., Mu, M., Saatchi, S., Santoro, M., Thurner, M., Weber, U., Ahrens, B., Beer, C., Cescatti, A., Randerson J. T., Reichstein M. (2014). Global covariation of carbon turnover times with climate in terrestrial ecosystems. Nature, 514, 213–217.

Coleman, K., & Jenkinson, D. S. (1999). RothC-26.3: A model for the turnover of carbon in soil: model description and Windows users guide. Lawes Agricultural Trust, Harpenden. ISBN: 0-951-4456-8-5. November 1999 issue.

Dorji, T., Field, D. J., Odeh, I. O. A. 2020. Soil aggregate stability and aggregate- associated organic carbon under different land use or land cover types. Soil Use Management, 36, 308–319.

Elliott, E. T. (1986). Aggregate structure and carbon, nitrogen, and phosphorus in native and cultivated soils. Soil Science Society of America Journal, 50, 627–633.

Gattinger, A., Muller, A., Haeni, M., Skinner, C., Fliessbach, A., Buchmann, N., Maeder, P., Stolze, M., Smith, P., Scialabba, E.H. Niggli, U. (2012). Enhanced top soil carbon stocks under organic farming. Proceeding of the National Academy of Sciences of the USA, 109, 18226-18231.

Gulde, S., Chung, H., Amelung, W., Chang, C., & Six, J. (2008). Soil carbon saturation controls labile and stable carbon pool dynamics. Soil Science Society of America Journal, 72, 605-612.

Guo, J.H., Liu, X.J., Zhang, Y., Shen, J. L., Han, W. X., Zhang, F., Christie, P., Goulding, K.W.T., Vitousek, P.M., Zhang, F.S. (2010). Significant Acidification in Major Chinese Croplands. Science, 327, 1008-1010.

Huesh, A., Bakkantyne, A., Cooper, L., Manera, M., Kimball, J., & Watts, J. (2017). The sensitivity of soil respiration to soil temperature, moisture, and carbon supply at the global scale. Global Change Biology, 23, 2090–2103.

Jamieson, P. D., Porter, J. R., & Wilson, D. R. (1991). A test of the computer simulation model ARC-WHEAT1 on wheat crops grown in New Zealand. Field Crops Research, 27, 337–350.

Jia Y, Kuzyakov Y, Wang G, Tan W, Zhu B, & Feng X. (2020). Temperature sensitivity of decomposition of soil organic matter fractions increases with their turnover time. Land Degrad Dev., 31, 632–645.

Lal, R. (2004). Soil carbon sequestration impacts on global climate change and food security. Science, 304, 1623–1627.

Li, N., You, M.Y., Zhang, B., Han, X.Z., Panakoulia, S.K., Yuan, Y.R., Liu, K., Qiao, Y.F., Zou, W.X., Nikolaidis, N.P., Banwart, S.A. (2017). Modeling soil aggregation at the early pedogenesis stage from the parent material of a Mollisol under different agricultural practices. Advances in Agronomy, 142, 181-214.

Lichter, K., Govaerts, B., Six, J., Sayre, K. D., Deckers, J., & Dendooven, L. (2008). Aggregation and C and N contents of soil organic matter fractions in a permanent raised-bed planting system in the Highlands of Central Mexico. Plant and Soil, 305, 237–252.

Liu, B., Gao, R., Ndzana, G.M., An, H., Huang, J., Liu, R., Du, L., Kamran, M., Xue B. (2023). Nutrient addition affects stability of soil organic matter and aggregate by altering chemical composition and exchangeable cations in desert steppe in northern China. Land Degradation and development, 34, 1430-1446.

Malamoud, K., McBratney, A. B., Minasny, B., & Field, D. J. (2009). Modelling how carbon affects soil structure. Geoderma, 149, 19–26.

Neff, J. C., Townsend, A. R., Gleixner, G., Lehman, S. J., Turnbull, J., & Bowman, W. D. (2002). Variable effects of nitrogen additions on the stability and turnover of soil carbon. Nature, 419, 915-917.

Panakoulia, S.K., Nikolaidis, N.P., Paranychianakis, N.V., Menon, M., Schiefer, J., Lair, G.J., Krám, P., Banwart, S.A. (2017). Factors Controlling Soil Structure Dynamics and Carbon Sequestration Across Different Climatic and Lithological Conditions. Advances in Agronomy, 142, 241-276.

Powlson, D. S., Whitmore, A. P., & Goulding, K. W. T. (2011). Soil carbon sequestration to mitigate climate change: A critical re-examination to identify the true and the false. European Journal of Soil Science 62, 42–55.

Qiu, S.J., He, P., Zhao, S.C., Li, W.J., Xie, J.G., Hou, Y.P., Grant, C.A., Zhou, W., Jin, J.Y. (2015). Impact of nitrogen rate on maize yield and nitrogen use efficiencies in northeast China. Agronomy Journal, 107: 305-313.

Ramteke, P., Gabhane, V., Kadu, P., Kharche, V., Jadhao, S., Turkhede, A., & Gajjala, R. C. 2024. Long- term nutrient management effects on organic carbon fractions and carbon sequestration in Typic Haplusterts soils of Central India. Soil Use Management, 40, e12950.

Schmidt, M.W. I., Torn, M.S., Abiven, S., Dittmar, T., Guggenberger, G., Janssens, I.A., Kleber, M., Kögel-Knabner, I., Lehmann, J., Manning, D.A.C., Nannipieri, P., Rasse, D.P., Weiner, S., Trumbore, S.E. (2011). Persistence of soil organic matter as an ecosystem property. Nature, 478, 49-56.

Six, J., Paustian, K. (2014). Aggregate-associated soil organic matter as an ecosystem property and a measurement tool. Soil Biology and Biochemistry, 68, A4-A9.

Six, J., Elliott, E. T., & Paustian, K. (2000). Soil macroaggregate turnover and microaggregate formation: A mechanism for C sequestration under no-tillage agriculture. Soil Biology and Biochemistry, 32, 2099-2103.

Stamati, F. E., Nikolaidis, N. P., Banwart, S., & Blum, W. E. H. (2013). A coupled carbon, aggregation, and structure turnover (CAST) model for topsoils. Geoderma, 211-212, 51-64.

Xiao, G., Hu, Y., Zhang, Q., Wang, J., & Li, M. (2020). Impact of cultivation on soil organic carbon and carbon sequestration potential in semiarid regions of China. Soil Use Management, 36, 83–92.

Yan, Y., Tian, J., Fan, M., Zhang, F., Li, X., Christie, P., Chen, H., Lee, J., Kuzyakov, Y., Six, J. (2012). Soil organic carbon and total nitrogen in intensively managed arable soils. Agriculture, Ecosystems and Environment, 150, 102-110.

Yu, H. Y., Ding, W. X., Luo, J. F., Geng, R. L., & Cai, Z. C. (2012). Long-term application of organic manure and mineral fertilizers on aggregation and aggregate-associated carbon in a sandy loam soil. Soil and Tillage Research, 124, 170-177.

Wang, J., Lu, C., Xu, M., Zhu, P., Huang, S., Zhang W., Peng, C., Chen, X., Wu, L. (2013). soil organic carbon sequestration under differnet fertilizer regimes in north and northeast China: RothC simulation. Soil use and management, 29, 182-190.

Wen, Y., Tang, Y., Wen, J., Wang, Q., Bai, L., Wang, Y., Su, S., Wu, C., Lv, J., Zeng, X. (2021). Variation of intra-aggregate organic carbon affects aggregate formation and stability during organic manure fertilization in a fluvo-aquic soil. Soil use and

management, 37, 151-163.
Zeller, B., & Dambrine, E. (2011). Coarse particulate organic matter is the primary source of mineral N in the topsoil of three beech forests. Soil Biology and Biochemistry, 43, 542-550.
Zhang, K., Dang, H., Zhang, Q., & Cheng, X. (2015). Soil carbon dynamics following land-use change varied with temperature and precipitation gradients: Evidence from stable isotopes. Global Change Biology, 21, 2762–2772.
Zhou M, Xiao Y, Zhang X, Xiao L, Ding G, Cruse RM, & Liu X. (2022). Fifteen years of conservation tillage increases soil aggregate stability by altering the contents and chemical composition of organic carbon fractions in Mollisols. Land Degrad Dev., 33, 2932–2944.
Zhou, X., Xu, X., & Luo, Y. (2018). Temperature sensitivity of soil organic carbon decomposition increased with mean carbon residence time Field incubation and data assimilation. Global Change Biology, 24, 810–822.

Table 1 Basic soil properties in the top 20 cm of the soil profile at the start of the experiment in 1986.

Soil property		Soil property	
Soil organic C (g kg^{-1})	9.4	pH	6.0
Total N (g kg^{-1})	1.0	Patent material	Quaternary red clay
Total P (g kg^{-1})	1.4	Soil texture	
Total K (g kg^{-1})	15.8	Sand (%)	21.2
alkali-hydrolyzable N (mg kg^{-1})	60.3	Clay (%)	27.6
Olsen-P (mg kg^{-1})	12.9	Silt (%)	51.2
NH_4Ac-K (mg kg^{-1})	102.0		

Table 2 Fertilizer rates in the control (CK), chemical fertilizer (CF), and combined manure and chemical fertilizer (MCF) treatments in each crop in the field experiment. Units: kg ha^{-1}

Crop	CK	CF	MCF		
	N:P:K	N:P:K*	N:P:K	Manure N	Manure C
Spring maize	0:0:0	60:13:50	60:13:50	141	1602
Summer maize	0:0:0	60:13:50	60:13:50	141	1602

*, Chemical fertilizer applied, not including manure nutrients.

Table 3 Measured SOC contents in 2014 and simulated SOC contents in 2014, simulated C inputs, simulated CO_2 emissions, and SOC sequestration rates by the RothC model in the control (CK), chemical fertilizer (CF), and combined manure and chemical fertilizer (MCF) treatments.

	Measured SOC ($t\ ha^{-1}$)	Simulated SOC ($t\ ha^{-1}$)	Simulated C input ($t\ C\ ha^{-1}\ yr^{-1}$)	Simulated CO_2-C emission ($t\ C\ ha^{-1}\ yr^{-1}$)	SOC sequestration rate* ($kg\ ha^{-1}\ yr^{-1}\ C\ input^{-1}$)
CK	20.2±1.2c	20.3±1.2c	2.6±0.3b	0.74±0.08b	-78.9±14.0c
CF	23.2±0.4b	23.1±0.3b	3.4±0.1b	0.92±0.02b	-30.9±4.8b
MCF	33.2±1.5a	33.2±1.6a	5.8±0.4a	1.47±0.10a	41.4±5.8a

NB: SOC, soil organic carbon

Means followed by a different letter within a column at each site are different at $P < 0.05$.

* Sequestration rate was that the difference between measured SOC between 2014 and 1986 divided the multiplication of simulated C input and experimental years.

Table 4 Water stable aggregate (WSA) mass and concentration at 0-20 cm soil depth in control (CK), chemical fertilizer (CF), and combined manure and chemical fertilizer (MCF) treatments in 2014.

WSA	Treatment	AC1[#]	AC2	AC3	AC2,3	AC1,3	AC1,2,3	cPOM	fPOM_inAC3
Mass	CK	6.0±0.6a	33.6±1.3a	59.3±2.1b	32.3±2.1a	20.9±0.5c	31.7±2.2a	0.60±0.08b	0.06±0.01b
(%)	CF	4.5±0.4b	29.1±1.1b	65.2±1.3a	34.3±1.4a	25.2±0.6b	33.8±1.4a	0.75±0.11b	0.09±0.02b
	MCF	4.1±0.4b	26.2±1.9b	68.2±2.2a	32.9±1.8a	29.3±1.3a	32.2±1.7a	1.26±0.15a	0.23±0.02a
C concentration	CK	0.44±0.04a	2.51±0.25a	4.42±0.31c	2.36±0.14c	1.27±0.08c	1.71±0.03c	0.62±0.06b	0.23±0.011c
($g\ kg^{-1}$)	CF	0.39±0.05a	2.37±0.09a	5.46±0.06b	3.07±0.12b	1.75±0.04b	2.41±0.06b	0.75±0.11b	0.27±0.008b
	MCF	0.41±0.06a	2.69±0.26a	8.26±0.26a	4.27±0.12a	2.38±0.13a	3.32±0.05a	1.29±a0.10	0.67±0.020a

NB:

[#]AC3, macroaggregates (> 250 μm); AC2, microaggregates (250-53 μm); AC, silt and clay (< 53 μm).

AC2,3, microaggregates in macroaggregates (250-53 μm); AC1,3, silt and clay in macroaggregates (< 53 μm).

AC1,2,3, silt and clay within microaggregates in macroaggregates (< 53 μm).

cPOM, coarse particulate organic matter; fPOM, fine particulate organic matter;

[†] Values are means of three replicates.

[‡] Means followed by a different letter within a column at each site are different at $P < 0.05$.

Table 5 Calibrated parameters (turnover time) of aggregate C at 0-20 cm soil depth in control (CK), chemical fertilizer (CF), and combined manure and chemical fertilizer (MCF) treatments using CAST model simulation.

	Parameter	CK	CF	MCF
Turnover time* (y)				
Fragmentation#	RPM	6.67	5.56	3.33
	RPMcinAC3	5.00	10.0	10.0
	DPMcinAC3	20.0	20.0	2.00
Macroaggregates §	RPMc	2.00	10.0	16.7
	DPMc	0.95	0.71	0.63
Microaggregates¶	RPMf$_{inAC2,3}$	14.3	16.7	5.00
	DPMf$_{inAC2,3}$	14.3	16.7	5.00
Plant litter pool decomposition	DPM	0.13	0.13	0.33
	RPM	322.6	3.28	3.28
	RPMc	5.00	10.0	5.00
	RPMf	3.28	3.28	3.28
AC3 aggregate type decomposition	RPMc$_{inAC3}$	3.33	6.67	10.0
	RPMf$_{inAC3}$	3.33	6.67	10.0
	DPMc$_{inAC3}$	0.33	0.28	0.36
	DPMf$_{inAC3}$	0.33	0.33	1.00
	BIO$_{inAC1,3}$	1.67	1.67	2.00
	HUM$_{inAC1,3}$	100.0	142.9	200.0
	BIO$_{inAC2,3}$	1.67	1.67	2.00
	HUM$_{inAC2,3}$	76.9	142.9	200.0
	RPMf$_{inAC2,3}$	1.97	40.0	48.3
	DPMf$_{inAC2,3}$	2.00	40.0	66.7
AC2 aggregate typedecomposition	BIO$_{inAC2}$	1.67	1.67	2.00
	HUM$_{inAC2}$	76.9	142.9	200.0
	RPMf$_{inAC2}$	4.83	4.83	48.3
	DPMf$_{inAC2}$	6.67	6.67	66.7
AC1 aggregate type decomposition	BIO$_{inAC1}$	1.67	1.67	1.00
	HUM$_{inAC1}$	5.00	2.50	2.00
Proportional contribution of the components in aggregation (%)				
Macroaggregates	RPMc	30.5	35.0	27.0
	DPMc	30.5	35.0	27.0
	AC1	23.0	18.0	22.0
	AC2	16.0	12.0	24.0
Microaggregates	RPMf$_{inAC3aggr}$	23.4	23.4	40.0
	AC1$_{inAC3}$	76.6	76.6	60.0
Correction factor for silt-clay mass flow (fraction)				
	AC1	0.60	0.65	0.90
	AC2	1.30	1.00	1.30
	AC1,3	0.80	1.20	1.20
Disruption criterion for aggregate distribution (%)				
DPM within AC3		0.0015	0.002	0.01
(DPM + RPM) inAC2,3		0.0015	0.002	0.01
(DPM + RPM) in AC2		0.0015	0.002	0.01
Tilling criterion for aggregate distribution (%)				
DPM within AC3		0.0035	0.0035	0.0035
(DPM + RPM) inAC2,3		0.0035	0.0035	0.0035
(DPM + RPM) in AC2		0.0035	0.0035	0.0035

Aggregate symbols: see the abbreviations indications.

NB: Aggregate symbols see the Abbreviations indications;

* Turnover time is calculated at the reciprocal value of the respective calibration rate constants (1/y) in CAST model;

\# Fragmentation refers to the decomposition of exogenous plant material;

§ Macroaggregate is coarse plant material mass transfer for macroaggregate formation;

¶ Microaggregate is fine plant material mass transfer for microaggregate formation within macroaggregate.

Table 6 RMSE and nRMSE of validation for soil organic C stock distribution between the measured value and simulated value using the CAST model in control (CK), chemical fertilizer (CF), and combined manure and chemical fertilizer (MCF) treatments in 2007.

WSA fraction	Treatment	Measured value ($tC\ ha^{-1}$)	Simulated value ($tC\ ha^{-1}$)	RMSE	nRMSE (%)
SOC	CK	21.9	20.3	1.6	7.4
	CF	24.4	23.2	1.2	4.8
	MCF	32.3	31.9	0.4	1.2
AC3	CK	12.1	11.9	0.3	2.3
	CF	16.0	15.4	0.6	3.8
	MCF	24.4	25.1	0.7	2.7
AC2	CK	8.7	7.4	1.3	14.6
	CF	7.2	6.8	0.4	5.1
	MCF	6.7	5.6	1.0	15.2
AC1	CK	32.3	31.9	0.1	11.7
	CF	1.3	1.0	0.2	17.2
	MCF	1.2	1.0	0.2	15.2

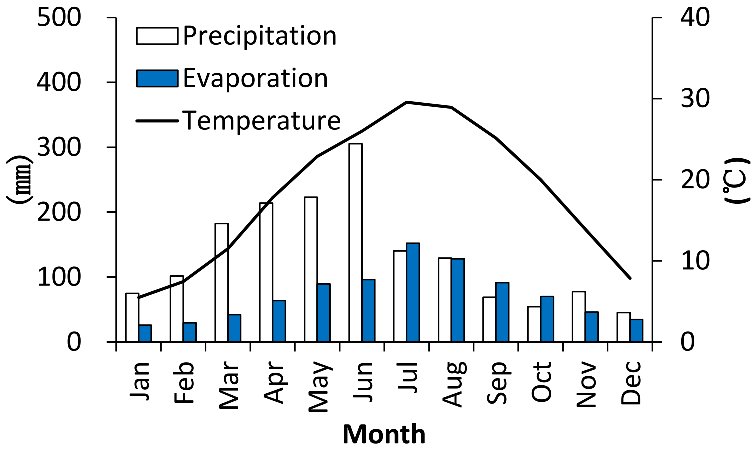

Fig. 1 Averaged monthly temperature, total monthly precipitation, and total monthly evaporation in Nanchang city, Henan province, during the period 1986-2014.

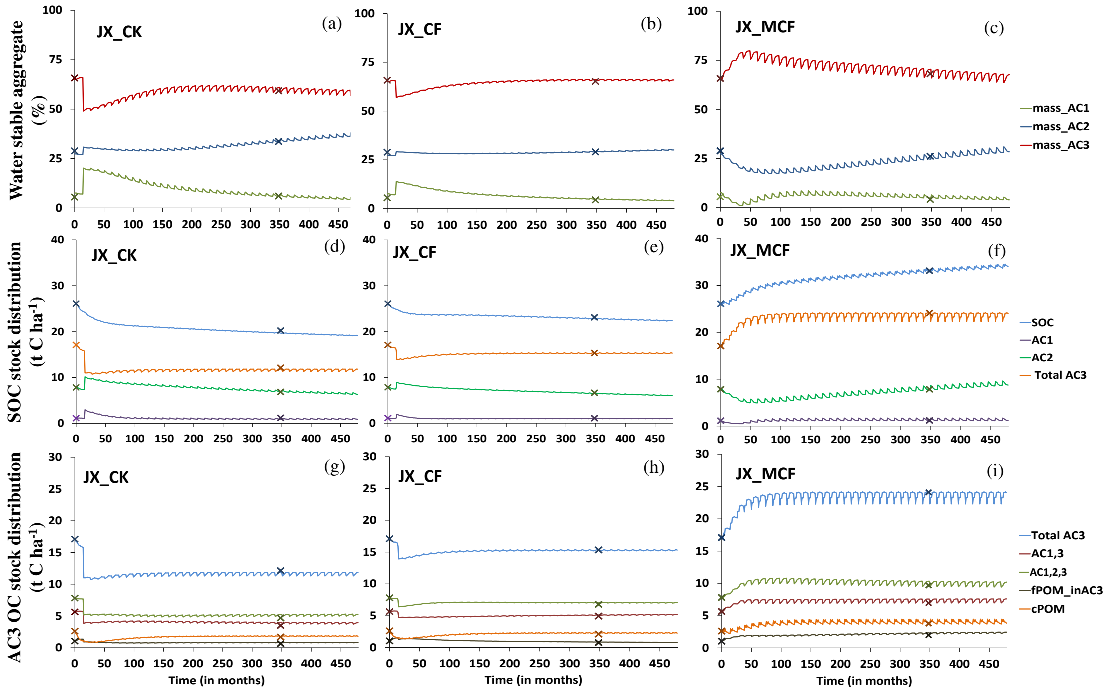

Fig. 2 Water stable aggregates (%), soil organic carbon (SOC) stock distribution, and macroaggregate (AC3) OC stock distribution as affected by fertilization treatment in control (CK), chemical fertilizer (CF), and combined manure and chemical fertilizer (MCF) treatments in Jiangxi (JX) province using CAST model simulation.

Aggregate symbols in legend: see Table 3 footnote.

Crosses in Figure are the measured values of the samples at the start of the experiment and in 2014.